Floren Radovanović-Perić[1], Ivana Panžić[1], Arijeta Bafti[1], Marko Rukavina[1], Andrea Jurov[1], Vilko Mandić[1]

Showcase of tools for preparing, modifying and describing thin films for energy conversion devices with special attention on plasma phenomenology

[1]Faculty of Chemical Engineering and Technology, University of Zagreb, Trg Marka Marulića 20, 10000 Zagreb, Croatia

Abstract

This paper draws attention to the wide range of capacities of the Group, including chemical and physical deposition, modification and processing techniques, and advanced characterisations. In particular, this work demystifies the new plasma discharge method for the synthesis of thin films, which is still under development. Specifically, the coupled spark plasma ablation deposition (SPAD) can be performed at almost ambient conditions in various configurations with respect to several deposition reactors, proving powerful, versatile, green, and easy-to-use nature of the method. Composition-wise, up to 4 element material can be derived combining pure electrodes, however the derived composition can be broader when using alloy electrodes. It is indisputable that SPAD is capable of producing thin films at a significantly reduced cost compared to other methods.which we want to put in use for the constituent layers of the last generation of energy conversion devices. Generally, the SPAD optimisation envelope heavily differs for the case of intended products: nanoparticle vs thin film, or metal vs metal oxide, or crystalline vs amorphous. Here, we will provide a more detailed description of the ablation parameters that are necessary to achieve the various crystallinities of nanomaterials. Copper nanoparticles and thin films were derived via SPAD and additionally thermally treated. (Micro)structural and thermal evolution points out to interesting development of the surface morphologies. In addition, the results enabled the correlation between oxygen plasma concentration and order of crystallinity in the thin films.

***Keywords**: spark ablation; plasma; nanomaterial; thin film; copper oxide.*

1. Introduction

Metallic and metal oxide nanoparticles attract considerable attention in various applications, such as biomedicine [1–3], optoelectronics [4], [5], energy conversion [6–9] and catalysis [10–12]. The quantum confinement effect and surface-to-volume ratio are the most interesting properties of metallic nanoparticles. Surface area, which increases with decreasing nanoparticle size, influences the interaction between nanoparticles and other reactive substances and consequently can enhance their performance in various applications. For some applications, such as energy conversion devices, it is useful to have nanoparticles in a thin film configuration. The necessary routes are covered within chemical and physical depositions, where the Group developed board expertise. Chemical depositions are more flexible and generally more economical, however they do not have the capability to modify the spatial delineation of the domains. A chemical deposition technique usually starts with some sort of solution chemistry process that has to be controlled to a desired time domain; from a long time domain for e.g. ambient humidity controlled yield of nanoparticles, to levels of short time domains for e.g. dip coating, to spin coating, to spray coating deposition of thin films. Generally, physical deposition techniques are often more specific, less economic, but quite precise. The Group developed expertise for all major thin film production techniques, including: magnetron sputtering (MS), thermal or e-beam evaporation (EBE), and pulsed laser deposition (PLD).

The ablation group of deposition technologies encompasses a wide range of chemical and physical processes, and are widely used in the synthesis of nanomaterials. There are two main ablation technologies available: laser ablation and spark-based ablation. These techniques are both green and efficient methods for nanomaterial synthesis. Spark plasma ablation deposition (SPAD) is based on the sudden sublimation of material from electrodes by inducing spark discharges between them, from which nanoparticles form by condensation [13]. Laser ablation is a highly studied and used technique, but it has certain disadvantages, such as the high cost and complexity of the setup [14]. To simplify the experimental setup, spark ablation is nowadays more often utilised. This type of ablation does not need a laser or vacuum, which reduces the cost of the procedure, is environmentally friendly as it needs no chemical precursors nor produces waste, and is highly scalable [15–16]. A spark discharge generator has a relatively simple design where the key components are two metal electrodes positioned with a small gap between them. Spark ablation is a technique where a metallic target, bombarded with high energy, loses localised atoms in the form of vapour and gives enough energy to the inert gas in its surroundings to form plasma. The inert gas in the state of plasma provides a clean environment for the formation of nanoparticles, and due to its rapid quenching effect, smaller nanoparticles can be formed [17]. In addition, in comparison with chemical methods for nanoparticle synthesis, spark ablation provides a clean synthesis with extremely high efficiencies and purity of the product, which depends only on the purity of the precursor.

The duration of the spark events that induce ablation may affect the size of the resulting particles. Smaller particles can be created by using shorter sparks. Also, shorter sparks help avoid continuous arcing, which would lead to effects like distillation that disable the possibility of producing mixed particles with controlled composition [15]. The size of the nanoparticles generated is typically less than 20 nm.

Another possibility with spark ablation is to easily produce mixed nanomaterials by using alloy electrodes. With different electrode configurations, it is possible to get an alloy of more than two materials. Additionally, this technique can produce ordered agglomerates and nanostructures consisting of more primary particle species. This is an ablation process specialty, as other nano-material synthesis techniques do not work at this scale to create mixtures. Another possibility is to coat or decorate produced particles [15].

Spark generation is a fast and short process that occurs when the breakdown voltage between the electrodes is reached. The breakdown voltage is quite high and depends on the gas pressure and inter-electrode gap. When the breakdown voltage is surpassed, the ionisation of the gas occurs along with increasing current, accompanied by an intense light emission – plasma. The formation of plasma is dependent on the electrical circuit and the gas in the environment and is capable of producing a variety of discharge types, including glows, arcs, sparks and corona [18]. The temporal evolution of sparks can be characterised by four stages – pre-breakdown, breakdown, arc and afterglow. All four stages have different physical characteristics and, consequently, different contributions to the ablation process [15]. Pre-breakdown and breakdown are dominated by gas emission; in pre-breakdown molecular bands are observed, whereas, in the breakdown, the main emitters are ions, followed by continuous radiation. The breakdown should complete rapidly, in less than 100 ns. The manifestation of a completed breakdown is the arc, which occurs when a conducting channel connects the electrodes. The arc stage is characterised by a large electrical current that heats the electrodes locally which leads to the ablation of the electrode material. This stage is optically defined by light emission of both the species from the ambient gas and electrode material. The arc usually occurs in less than a microsecond after the breakdown. Lastly, there is an afterglow stage where the light emission does not cease even after the current terminates. This emission comes from the metastable species of the ambient gas lingering in and around the spark gap, characterised by lower gas temperature and lower pressure. The afterglow stage can last between tens of microseconds and a couple of milliseconds if another spark has not occurred. The most important stages for nanoparticle production are the arc and the afterglow because most material is ablated during arcing, and the formation of nanoparticles takes place in the afterglow.

However, while spark ablation holds great potential in all fields of nanoparticle research, there is still much work to be done in order to fully understand the effects of process parameters on each oxidation state, phase, particle size distribution, morphology and nanoporosity of the deposited materials.

Thanks to their chemical stability and non-toxicity, copper oxide (Cu_xO_y) nanostructured thin films have recently found many useful applications as low-cost materials in energy conversion fields. Stable Cu_xO_y phases include Cu_2O (cuprite) and CuO (tenorite), while there are numerous metastable phases, amongst them Cu_4O_3 (paramelaconite), an oxide of copper intermediate between the two, corresponding to the formula $Cu_2O{\cdot}(CuO)_2$. CuO and Cu_2O films are generally believed to be p-type semiconductors with band gap energies in visible and near-infrared regions [19]. Moreover, they have high absorption coefficients making them highly promising candidates for active layers in solar cells [20], optoelectronic detectors [21] or sensors [22].

Nanostructured copper oxide thin films can be prepared by several methods: sol-gel, magnetron sputtering, thermal oxidation, hydrothermal, spray pyrolysis, microwave-assisted etc. While all these methods can produce different morphologies and nanostructures, their main disadvantage is expensive equipment to achieve ultra-high vacuum or controlled heating and cooling steps, expensive reagents or low reproducibility. Thin metallic oxide films produced by reactive spark ablation ensure high purity of the material and can be prepared easily in the nanometre range by introducing oxygen into the gas flow. The oxygen reacts with the nanoparticles immediately after their creation. Theoretically, complete conversion is possible at room temperature, in contrast to the commonly used chemical syntheses, which require thermal treatment after deposition.

From the aforementioned, it is obvious that SPAD is one of the few methods that are capable of producing stable metallic oxide nanosized thin films at both ambient temperature and pressure in a time range spanning from no more than a few seconds to a few minutes. In this segmental study, we will focus on the characterisation of the as-prepared thin films at room temperature derived by spark ablation and after their thermal evolution to CuO.

2. Materials and methods

The following materials and chemicals were used: Copper electrodes (6 mm thickness, 99.9% purity, VSParticle, Delft, Netherlands), isopropanol (p.a. Lachner, Zagreb, Croatia).

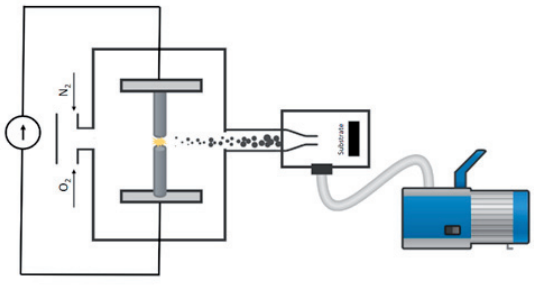

Figure 1. Schematic representation of the SPAD system setup for copper oxide synthesis and subsequent thin film formation.

For the purpose of this research, spark plasma ablation deposition (SPAD) was configured in a crossflow vacuum-assisted impaction deposition setup depicted by the scheme below (**Figure 1**, model, VSParticle, Delft, Netherlands). Two gases, a carrier gas (nitrogen) and a reactive gas (oxygen), are introduced into the reactor containing two copper electrodes. After reaching the breakdown voltage, nanoparticle formation and copper oxidation occur, and the particles are carried away from the electrodes to the deposition chamber. Before reaching the nozzle, the aerosol flow is concentrated and accelerated by narrowing the tube diameter. Upon reaching the vacuum chamber, the aerosol gains a significant kinetic energy boost due to the difference in pressures between the reaction and deposition chamber. The width of the aerosol jet upon impaction is controlled by nozzle width, chamber vacuum pressure (2-200 mbar) and substrate to nozzle distance. Spark discharge was performed in two extremely different atmospheres; 0.07 slpm and 1.05 slpm of oxygen in a total flow of 10 slpm. Thin films were deposited on Si wafers that were previously immersed in isopropanol in an ultrasonic bath for 15 minutes and then exposed to ozone for 15 minutes to remove all of the organic waste at the surface.

Grazing incidence X-ray diffraction was used to study and characterize the thin film crystal structure and its thermal evolution. Patterns were collected using synchrotron radiation (MCX beamline of the Elettra Synchrotron Trieste) using 4-axis Huber goniometer, at 10 keV, step 0.02° 2theta, retention time 0.7 sec in a 2θ range of 5–70° with at grazing angle of 0.5 theta.

Particle and thin film morphologies were observed by two scanning electron microscopes (SEM, Prisma E, Thermo Fisher Scientific Inc., Massachusetts, USA; and JSM 700F, Jeol Ltd., Akishima, Tokio, Japan).

Gas-phase analysis of plasma was conducted by optical emission spectroscopy with a broad-range spectrometer (model LR1, ASEQ Instruments, Vancouver, Canada).

3. Results and discussion

3.1. Plasma analysis

The gas phase plasma diagnostic was conducted with optical emission spectroscopy – a simple tool that has the ability to identify excited species inside the plasma. This method allows one to pinpoint atomic transitions that possibly participate in nanoparticle formation. **Figure 2** presents emission spectra taken during copper ablation with two gas mixtures of nitrogen and oxygen. Nitrogen gas flow was fixed at 10 slpm, but oxygen gas flow was varied between a lower flow of 0.07 slpm and a higher flow of 1.05 slpm.

Both spectra show the same excited atomic species of copper (Cu i from 325 to 329 nm, and Cu ii from 248 to 302 nm), nitrogen (N i, N ii, and N iii from 325 to 940 nm) and oxygen (O i from 715 to 927 nm). The lack of molecular bands in the OES indicates high plasma temperature, as it takes a lot of energy to break molecular bonds and ionize atoms. The main difference between spectra taken for different oxygen flow concentrations is in the emission intensity of all present excited species. For higher oxygen gas flow of 1.05 slpm, emission intensities are also higher, implying that the oxygen concentration in the gas mixture is directly responsible for the excitation of all present plasma species.

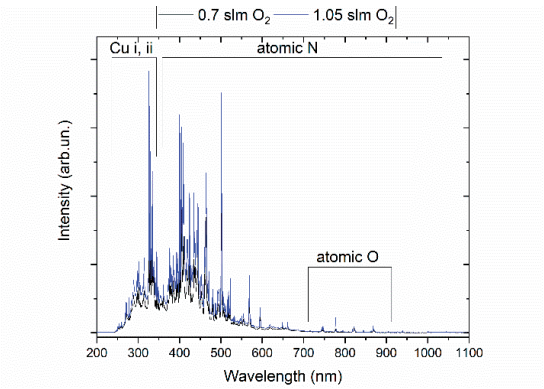

Figure 2. Optical emission spectra of plasma during nanoparticle synthesis for gas mixtures of N_2 and O_2 with line analysis

3.2. Structural ordering and potential for lattice oxygen defect engineering

Diffractograms in **Figure 3** show a crystalline film even at room temperature, where copper and cuprite phases are present. With increasing temperature, the film oxidizes, with a cuprite/tenorite mixed phase system being present at 160 °C, where cuprite is the dominant phase, which can be concluded from the intensity of the Cu_2O diffraction maxima. The cuprite phase further oxidizes, leading to a tenorite dominant phase at 350 °C. However, even at 350 °C, where complete oxidation to tenorite for nanosized copper is expected, the oxidation is incomplete, indicating a fair amount of aggregation [23].

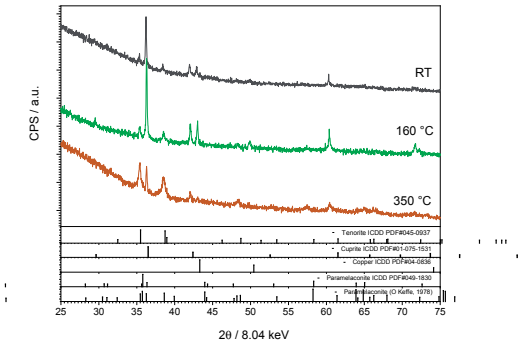

Figure 3. GIXRD patterns of thin films synthesized at 0.07 slpm O_2 thermally treated to various temperatures.

Figure 4 shows patterns of completely amorphous thin films at room temperature. The thermal treatment triggers oxidation, following the same evolutionary pathway as for the sample deposited with a lower amount of oxygen. A mixed tenorite/cuprite phase appears at an intermediate temperature, finally reaching a dominant tenorite system at 350 °C. In both samples, various unidentified diffraction peaks appear, which can all be contributed to mainly paramelaconite phases and a variety of copper oxides with more complex stoichiometries (Cu_xO_y). This is a characteristic of reactive plasma processes where condensation, oxidation and particle formation occur very fast without a solvent, which results in a somewhat uncontrollable process. Generally, during very high local temperatures reached during sparking (~15 000 K), one can expect the formation of only the most thermodynamically favoured phases. However, we show that metastable phases, such as cuprite, paramelaconite and other complex oxides, can be trapped with finely tuned spark and physical deposition parameters. These can all be described as one unique and useful feature spark plasma can provide in nanomaterial synthesis – oxygen lattice defects. These defects are related to the nature of oxygen plasma (a variety of oxygen ion species) inside the reactor and its concentration. It can be said that with increasing the amount of oxygen, more vacancies and defects are introduced into the lattice, resulting in a highly disordered structure, as can be seen for as-synthesized thin films at higher flow rates of oxygen.

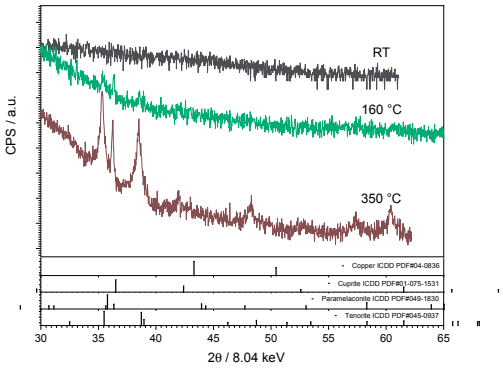

Figure 4. GIXRD patterns of thin films synthesized at 1.05 slpm O_2 thermally treated to various temperatures.

3.3. Particle morphology and thin film formation

Figure 5 and **Figure 6** show micrographs of samples deposited at room temperature and then thermally treated to 160 °C and 350 °C. As-synthesized samples show a small amount of distinguishable particles embedded in a poorly crystalline matrix. Further increase in temperature triggers crystallization with the appearance of triangle-shaped, sharp-edged crystals with a wide size distribution ranging from a few hundred nanometres to a few micrometres. The sharp-edged geometry of the crystals implies that these can be attributed to the cuprite phase. Upon reaching a higher temperature, the most prominent crystals show spherical-like morphology, generally observed in systems where the dominant tenorite phase exists [24].

Furthermore, with the increase in temperature, the order of crystallinity visibly increases for both samples, and agglomeration occurs. However, generally one can observe that the film is non-uniform and that the particles are distinguishable from one another, exhibiting high apparent surface roughness. This is a consequence of the kinetic energy of particle impaction onto the substrate. Namely, this is a function of the pressure ratio between the reactor and the deposition chamber (p_1/p_2), which can be considered a power coefficient for the efficiency of the deposition; the bigger the difference, the higher the kinetic energy of the aerosol.

Critical kinetic energy must be reached for the particles to plastically deform onto the substrate, forming a dense nanoporous film. Otherwise, nanoparticles exhibit elastic behaviour and form a structure that can be considered more of a powder than a thin film. An aerosol influx of

10 slpm into the deposition chamber limits the minimum pressure in the chamber to ~200 Pa, which significantly reduces the power factor and deposition efficiency and affects the thin film formation. By reducing the nozzle size, a lower nominal aerosol flux can be used for deposition, lowering the minimum pressure limit by about two orders of magnitude (~2 Pa). As the power factor increases by roughly two orders of magnitude, so does the kinetic energy, which significantly shifts the morphology of the sample/thin film. This is best displayed in **Figure 7**, where in comparison to **Figure 5** and **Figure 6**, the film is uniform and shows porosity only on a meso-nanoscale. Moreover, no singular particles are formed on the surface, and the film appears to be of uniform phase.

For this investigation, copper oxide nanoparticles were synthesized, deposited onto a substrate and thermally treated to obtain a tenorite-dominated thin film at 350 °C. During the course of the study, appropriate chemical analysis was carried out on the plasma gas phase and on the synthesized materials.

Plasma diagnostic did not detect any difference in plasma composition with respect to the oxygen content in the gas mixture but rather the change in intensity. It was discovered that adding more oxygen results in less structurally organized material; yet, all of the samples crystallized equally in terms of temperature.

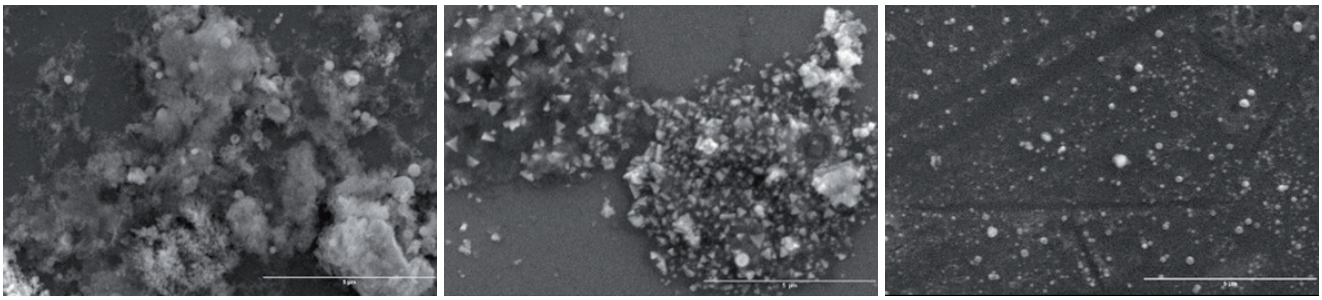

Figure 5. SEM micrographs of Cu_xO_y prepared with a mixture of 10 slpm nitrogen and 0.7 slpm oxygen (from left to right: 30 °C, 160 °C, 350 °C).

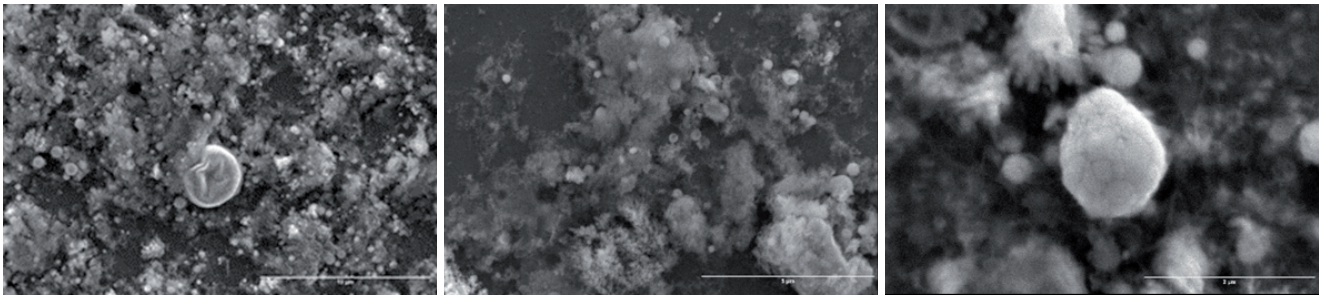

Figure 6. SEM micrographs of Cu_xO_y prepared with a mixture of 10 slpm nitrogen and 1.05 slpm oxygen (from left to right: 30 °C, 160 °C, 350 °C).

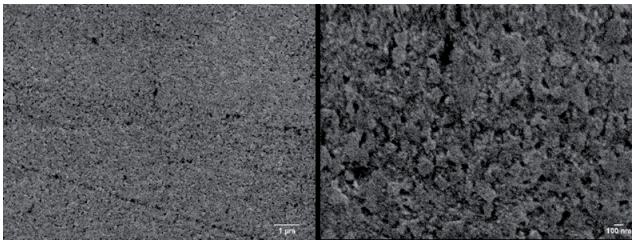

Figure 7. SEM micrographs of thin films of copper oxide nanoparticles deposited at 0.07 slpm O_2 and 1 slpm total flow through a smaller nozzle and lower chamber pressure (~2 Pa).

4. Conclusion

SPAD (Spark Plasma Ablation Deposition) setup can be used both as a nanoparticle synthesis method and as a nanoparticle deposition method. In any case, SPAD can produce lattice defects not only on the thin film's surface but also throughout the material.

To sum up, we demonstrate the ability to control the crystallinity range of synthesized materials through SPAD setup, through appropriate selection of ablation parameters (gas composition and flow) and post synthesis treatments.

5. References

[1] M. Nikzamir, A. Akbarzadeh, and Y. Panahi, "An overview on nanoparticles used in biomedicine and their cytotoxicity," *J. Drug Deliv. Sci. Technol.*, vol. 61, p. 102316, Feb. 2021

[2] A. Jurov *et al.*, "Atmospheric pressure plasma jet–assisted impregnation of gold nanoparticles into PVC polymer for various applications," *Int. J. Adv. Manuf. Technol.*, vol. 101, no. 1–4, pp. 927–938, Mar. 2019

[3] B. Farkaš and N. H. de Leeuw, "A Perspective on Modelling Metallic Magnetic Nanoparticles in Biomedicine: From Monometals to Nanoalloys and Ligand-Protected Particles," *Materials (Basel).*, vol. 14, no. 13, p. 3611, Jun. 2021

[4] J. Ma and S. Gao, "Plasmon-Induced Electron–Hole Separation at the Ag/TiO_2 (110) Interface," *ACS Nano*, vol. 13, no. 12, pp. 13658–13667, Dec. 2019

[5] T.-H. Lee, J. I. Gonzalez, J. Zheng, and R. M. Dickson, "Single-Molecule Optoelectronics," *Acc. Chem. Res.*, vol. 38, no. 7, pp. 534–541, Jul. 2005

[6] P. Matheu, S. H. Lim, D. Derkacs, C. McPheeters, and E. T. Yu, "Metal and dielectric nanoparticle scattering for improved optical absorption in photovoltaic devices," *Appl. Phys. Lett.*, vol. 93, no. 11, p. 113108, Sep. 2008

[7] H. A. Atwater and A. Polman, "Plasmonics for improved photovoltaic devices," *Nat. Mater.*, vol. 9, no. 3, pp. 205–213, Mar. 2010

[8] K. R. Catchpole and A. Polman, "Design principles for particle plasmon enhanced solar cells," *Appl. Phys. Lett.*, vol. 93, no. 19, p. 191113, Nov. 2008

[9] S. Pillai, K. R. Catchpole, T. Trupke, and M. A. Green, "Surface plasmon enhanced silicon solar cells," *J. Appl. Phys.*, vol. 101, no. 9, p. 093105, May 2007

[10] W. Kang, C. Cheng, Z. Li, Y. Feng, G. Shen, and X. Du, "Ultrafine Ag Nanoparticles as Active Catalyst for Electrocatalytic Hydrogen Production," *ChemCatChem*, vol. 11, no. 24, pp. 5976–5981, Dec. 2019

[11] C. Gao, F. Lyu, and Y. Yin, "Encapsulated Metal Nanoparticles for Catalysis," *Chem. Rev.*, vol. 121, no. 2, pp. 834–881, Jan. 2021

[12] X. Li, X. Hao, A. Abudula, and G. Guan, "Nanostructured catalysts for electrochemical water splitting: current state and prospects," *J. Mater. Chem. A*, vol. 4, no. 31, pp. 11973–12000, 2016

[13] T. V. Pfeiffer, J. Feng, and A. Schmidt-Ott, "New developments in spark production of nanoparticles," *Adv. Powder Technol.*, vol. 25, no. 1, pp. 56–70, 2014

[14] A. Voloshko and T. E. Itina, "Nanoparticle Formation by Laser Ablation and by Spark Discharges — Properties, Mechanisms, and Control Possibilities," *Nanoparticles Technol.*, pp. 1–12, 2015

[15] A. Schmidt-Ott, Ed., *Spark Ablation*, 1st ed. New York: Jenny Stanford Publishing, 2020.

[16] M. Stein and F. E. Kruis, "Scaling-up metal nanoparticle production by transferred arc discharge," *Adv. Powder Technol.*, vol. 29, no. 12, pp. 3138–3144, Dec. 2018

[17] J. Lu *et al.*, "Preparation of Ag nanoparticles by spark ablation in gas as catalysts for electrocatalytic hydrogen production," *RSC Adv.*, vol. 10, no. 63, pp. 38583–38587, 2020

[18] E. Hontañón *et al.*, "The transition from spark to arc discharge and its implications with respect to nanoparticle production," *J. Nanoparticle Res.*, vol. 15, no. 9, 2013

[19] M. Arreguín-Campos *et al.*, "Synthesis of paramelaconite nanoparticles by laser ablation," *J. Laser Appl.*, vol. 30, no. 1, p. 012012, 2018

[20] T. K. S. Wong, S. Zhuk, S. Masudy-Panah, and G. K. Dalapati, "Current status and future prospects of copper oxide heterojunction solar cells," *Materials (Basel).*, vol. 9, no. 4, pp. 1–21, 2016

[21] H. J. Song, M. H. Seo, K. W. Choi, M. S. Jo, J. Y. Yoo, and J. B. Yoon, "High-Performance Copper Oxide Visible-Light Photodetector via Grain-Structure Model," *Sci. Rep.*, vol. 9, no. 1, pp. 1–10, 2019

[22] S. Aghajani, A. Accardo, and M. Tichem, "Aerosol Direct Writing and Thermal Tuning of Copper Nanoparticle Patterns as Surface-Enhanced Raman Scattering Sensors," *ACS Appl. Nano Mater.*, vol. 3, no. 6, pp. 5665–5675, 2020

[23] S. Choudhary *et al.*, "Oxidation mechanism of thin Cu films: A gateway towards the formation of single oxide phase," *AIP Adv.*, vol. 8, no. 5, 2018

[24] Y. Alajlani *et al.*, "Characterisation of Cu_2O, Cu_4O_3, and CuO mixed phase thin films produced by microwave-activated reactive sputtering," *Vacuum*, vol. 144, pp. 217–228, 2017